Dynamic Analysis of Flexible-Joint and Single Flexible-Link Manipulator by Using Finite Element Analysis

Rajesh Ranjan, Saleendra Hari Babu, and Santosha Kumar Dwivedy

Abstract To improve productivity by operating the robotic manipulators at a higher speed, one may use a flexible-link manipulator. Sometimes, the joints of the manipulator can also be considered flexible. However, these flexible links and joints create unwanted vibration which reduces the efficacy of the manipulators. Due to this, many researchers are working to study the dynamics of these systems to reduce the problem of vibration in the systems. The present work focuses on the dynamic modeling and modal analysis of a cantilever beam-based curved flexible single link and joint manipulator. The analyses are carried out by using finite element analysis software ANSYS. The effects of joint and link flexibility on the system frequencies have been investigated. In the analyses, rectangular and tapered cross-sections for the links are considered. Furthermore, the findings of this study are compared to those of previous experimental studies published in the literature.

Keywords Curved flexible link · Flexible joint · Mode shapes · Natural frequencies

Nomenclature

a	Width of the tapered link at the left end
b	Width of the tapered link at the right end
B	Width of the link
E	Young's modules

R. Ranjan (✉) · S. H. Babu
Department of Mechanical Engineering, GITAM Deemed to Be University, Bangalore PIN-561203, India

S. H. Babu
e-mail: saleendr@alumni.iitg.ac.in

S. K. Dwivedy
Department of Mechanical Engineering, IIT Guwahati, Assam 781039, India
e-mail: dwivedy@iitg.ac.in

R. Tiwari et al. (eds.), *Vibration Engineering and Technology of Machinery, Volume I*, Mechanisms and Machine Science 137, https://doi.org/10.1007/978-981-99-4721-8_33

H Thickness of the link
I Moment of inertia
J_r Rotor inertia
J_a Payload of mass moment of inertia
K Joint stiffness
L Length of the flexible link
M_p Payload mass
N Shape function
r Radius of the hole
τ_0 External torque
α Angle of link
ρ Density of material

1 Introduction

In recent years, the research on lightweight flexible manipulators has seen heightened interest in the scientific community. The flexible manipulators have the advantages of higher operational speed, large working volume with greater payload-to-manipulator-weight ratio, and low cost. However, they suffer from their inherent flexibilities that need to be tackled in order to effectively utilize their potential advantages. The link and joint flexibilities are the two main reasons for the vibration of light manipulators, which can be proved costly to neglect them in dynamic modeling of the manipulator. A common method of dynamic modeling of a flexible robot manipulator for controller design is to use the Euler–Lagrange formulation with the assumed mode method, which gives the dynamic model of the manipulator in closed form. Most of the studies of flexible-link manipulators (FLMs) in the literature have considered the flexible links of manipulators as the Euler–Bernoulli beam.

Extensive research has been carried out on the modeling and the control of flexible manipulators. Dwivedy and Eberhard [1] reviewed the literature for the period 1974 to 2005 on dynamic analysis of flexible manipulators and classified them based on the study of manipulators with a different number of flexible links, methods used for dynamic analysis, and the control techniques applied. Kiang et al. [2] did a survey of the control techniques used in controlling the flexible manipulators during the period from 1990 to 2002. Ankarali and Diken [3] did the vibration control of an elastic link of a manipulator. Wang and Guan [4] examined the effects of different payload masses on the fundamental frequencies of flexible manipulators. They found that shear deformation and rotary inertia of the flexible link don't have much effect on the fundamental frequency of vibration. Wang and Russell [5, 6] applied the shape optimization techniques for vibration control of a flexible manipulator. KhalilIbrahim et al. [7] did the mode shape analysis of a single-link flexible manipulator. Shin and Brennan [8] applied control algorithms for residual vibration control of flexible manipulators based on the shock response spectrum. Korayem and Nikoobin [9],

Malgaca and Karagülle [10], and Malgaca et al. [11] used the finite element method for residual vibration control of flexible-link flexible-joint manipulators. De Luca and Siciliano [12] did the trajectory control of a single-link flexible manipulator. Abe [13] used the particle swarm optimization technique for trajectory planning for the residual vibration control of a two-link rigid–flexible manipulator. The flexible joint of the manipulator was modeled as a linear spring by Spong [14]. Wei et al. [15] applied the optimal trajectory planning for eliminating the residual vibrations of a rigid–flexible two-link manipulator with a flexible joint.

The main objective of the present work is to carry out the dynamic analysis of different shapes of flexible links with or without flexible joints using the finite element method. Here, five types of manipulators have been considered, viz., (1) rigid-joint and flexible-link manipulator with a rectangular cross-section, (2) rigid-joint and flexible-link manipulator with rectangular holes, (3) rigid-joint and tapered flexible-link manipulator, (4) single flexible-link flexible-joint manipulator, and (5) curved flexible-fink and rigid-joint manipulator with circular holes. In these works, the modal frequencies of the manipulators have been found out using the ANSYS software package.

2 Modeling

Figure 1 shows the model of a rigid-joint and flexible-link manipulator. Initially, this 3D model is developed by using SOLIDWORKS software. Here, the parameters considered for the flexible link are ($L \times H \times B$) = (0.5 × 0.05 × 0.003 m) and the initial curvature angle is $\theta = 30^0$, mass per unit length is 0.403 kg/m, bending stiffness ($EI = 7.85$ N.m^2), and tip payload mass $Mp = 0.5$ kg. Figure 2 shows the SOLIDWORKS model of the rigid-joint and flexible-link manipulator with circular holes. Here, the hole diameter is $d = 10$ mm, and the remaining parameters are the same as in Fig. 1. Figure 3 shows the rigid joint and tapered flexible-link manipulator having $a = 0.05$ m at the left end and $b = 0.025$ m at the right end, and the remaining parameters are the same as in the first case. Figure 4 shows an ANSYS model of a curved flexible-link and rigid-joint manipulator with circular holes, and physical parameters for this manipulator are given in Table 1. Figure 5 shows a schematic diagram of a flexible-joint and flexible-link manipulator. Here parameters considered are flexible link length ($L = 0.5$ m), width of the planar link ($B = 0.03$ m), thickness of the link ($H = 0.0015$ m), density of the material of the link (7800 kg/m^3), Young's modulus ($E = 200$ GPa), and joint stiffness (torsional spring constant $K_s = 750$ N.m/rad). It may be noted that the flexible joint is modeled as a torsional spring with stiffness K_s as shown in Fig. 5.

Finite element modeling has been carried out in ANSYS by exporting the SOLIDWORKS model (Figs. 1, 2 and 3) for the first 3 cases and in the last 2 cases, the models have been developed in ANSYS itself. Three-dimensional 4-noded tetrahedron solid structural elements have been considered in these models. The total number of elements and nodes used in the 5 different cases is given in Table 2. In

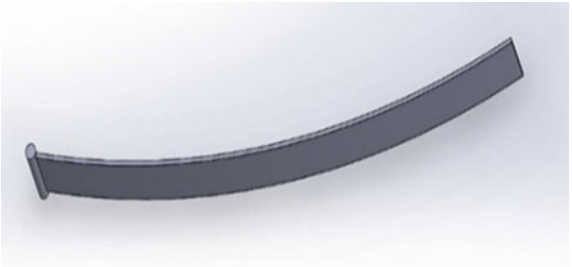

Fig. 1 SOLIDWORKS model of rigid-joint and flexible-link manipulator with a rectangular cross-section

Fig. 2 Rigid-joint and flexible-link manipulator with circular holes

Fig. 3 Rigid-joint and tapered flexible-link manipulator

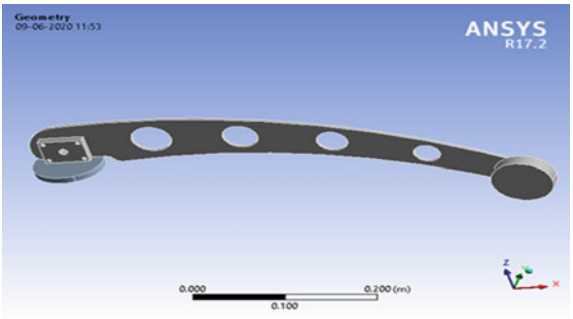

Fig. 4 ANSYS model of curved flexible-link and rigid-joint manipulator with circular holes

Table 1 Physical parameters of curved flexible-link and rigid-joint manipulator with circular holes

S. No.	Description	Curved manipulator
1	Young's modulus of elasticity	$E = 193$ GPa
2	Density	$\rho = 7950$ kg/m^3
3	Length	$L = 520$ mm
4	Distance of the payload from the end point	$d_{\text{payload}} = 20$ mm
5	Distance of the accelerometer center from the center of the payload	$d_{sensor} = 70$ mm
6	Thickness	$h = 4$ mm
7	Number of finite elements	$n_e = 2229$
8	Rayleigh damping coefficient	$\beta = 3.8 \times 10^{-4}$
9	Weight of the sensor	$M_s = 0.054$ kg
10	Weight of the payload	$M_L = 0.62$ kg
11	Motor rotational spring constants	$K_{m2} = 16{,}000$ Nm/rad
12	Time step	$\Delta t = 0.005$ s

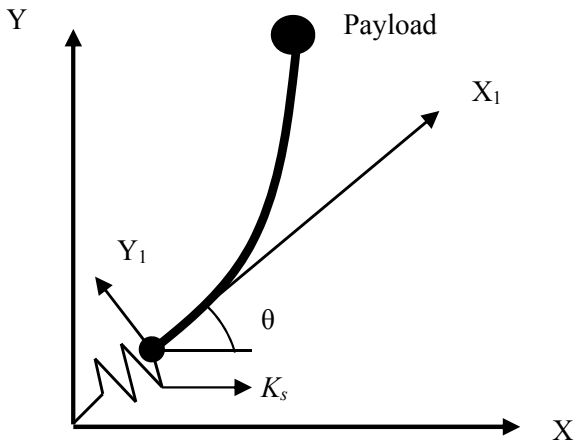

Fig. 5 Schematic diagram of flexible-joint and flexible-link manipulator

the first 4 cases, the left end of the manipulator is considered to be clamped and the other end is considered to have tip mass. In the fifth case, the left end is provided with a torsional spring and the other end is similar to the previous cases.

Table 2 Mesh-generated total elements and total nodes

Case	Modal name	Elements	Nodes
1	Rigid-joint and flexible-link manipulator with a rectangular cross-section	658	1569
2	Rigid-joint and flexible-link with holes manipulator system	877	2058
3	Rigid-joint and tapered flexible-link manipulator system	558	2032
4	Flexible-joint and flexible-link manipulator system	1378	5292
5	Curved flexible-link and rigid-joint manipulator with circular holes	528	2008

3 Results and Discussion

3.1 Dynamic Analysis of Flexible-Link and Rigid-Joint Manipulator

Modal analysis has been carried out in ANSYS and the mode shapes for the flexible link with rigid-joint manipulators are shown in Figs. 6 and 7 for 0 kg (no payload condition) and 0.5 kg payload, respectively. Here, the first 2 modes have been considered. The first 3 modal frequencies are given in Table 3 and are compared with those values available in the literature (KhalilIbrahim et al. [7]). The difference in the modal frequencies is found to be very less. It is clearly observed that by increasing the payload the modal frequencies are decreasing.

Now by making holes in the flexible links, Fig. 8 shows the first two modes of the manipulators with rigid joints. The modal frequencies are found to be 9.72 and 58.38 Hz which are more than those found in the first case (i.e., without holes). So by appropriately incorporating holes in the manipulator, one may control the tip deflection.

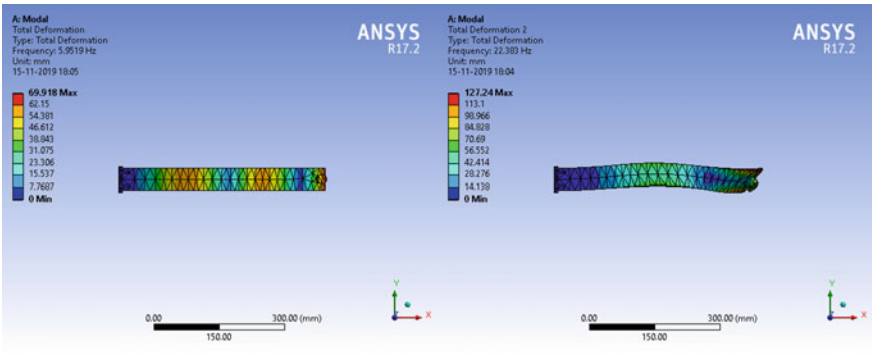

Fig. 6 Rectangular flexible-link and rigid-joint mode shapes of Mp = 0 kg

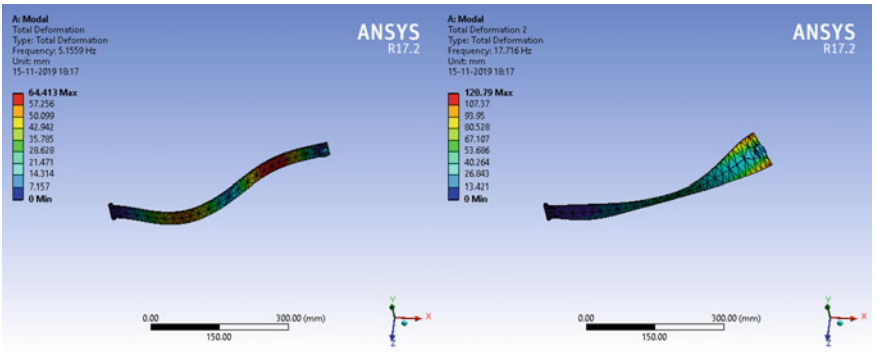

Fig. 7 Mode shapes of rectangular flexible-link and rigid-joint manipulator with $Mp = 0.5$ kg

Table 3 Modal frequencies of manipulator of rectangular flexible-link and rigid-joint with various payloads

Mode Shape no	Mode frequencies (Hz)					
	$Mp = 0\ kg$		$Mp = 0.25\ kg$		$Mp = 0.5\ kg$	
	[7]	Present work	[7]	Present work	[7]	Present work
1	7.97	5.95	6.92	5.29	6.31	5.15
2	23.973	22.38	18.35	18.44	15.17	17.716
3	64.501	63.201	49.37	51.86	44.76	45.1

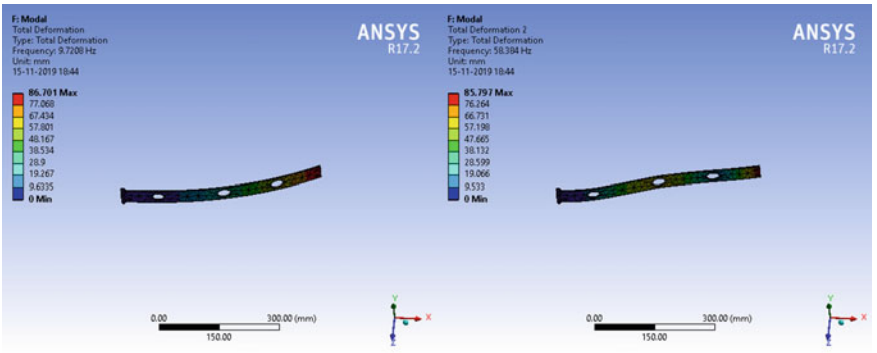

Fig. 8 Mode shapes of rectangular flexible-link and rigid-joint manipulator with holes and $Mp = 0$ kg

Figure 9 shows the first 2 mode shapes of the system shown in Fig. 3 where the link is considered to be tapered. Here, the modal frequencies are found to be 12.635 and 67.337 Hz which are more than those found in the first two cases. These values are found to be more than those of the first 2 cases.

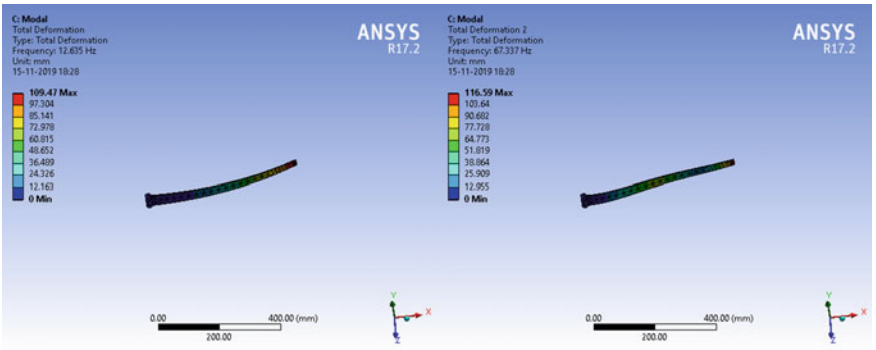

Fig. 9 Mode shapes of tapered flexible-link manipulator with $Mp = 0$ kg

Table 4 Comparison of modal frequencies of flexible-link and rigid-joint manipulator with other different shapes of flexible links

Model no.	Modal frequency (Hz)					
	$Mp = 0$ kg			$Mp = 0.5$ kg		
	Case 1	Case 2	Case 3	Case 1	Case 2	Case 3
1	5.95	9.728	12.635	5.15	5.3538	5.8175
2	22.38	58.384	67.337	17.716	29.624	29.816
3	63.201	71.432	91.793	45.1	47.596	49.351

Table 4 gives the comparison of the first 3 modal frequencies of the above-mentioned 3 cases of flexible-link and rigid-joint manipulators. One may choose the manipulators based on applications and kinematic constraints. The manipulators must operate away from the modal frequencies to avoid excessive vibration due to resonance.

3.2 Dynamic Analysis of Flexible-Joint and Flexible-Link Manipulator

The manipulator shown in Fig. 5 is analyzed in this subsection. FEA simulation has been carried out on a single flexible-link and flexible-joint manipulator with the joint torsional stiffness $K_s = 750$ Nm/rad. In Fig. 10, the first mode of vibrations of the flexible-link flexible-joint manipulator has been shown while in Fig. 11, the second mode of vibrations of the manipulator has been shown. In each of these cases, frequencies of the flexible-link and flexible-joint manipulators are calculated from their equilibrium position.

The frequencies for the first three modes of vibrations of the flexible-link and flexible-joint manipulator have been given in Table 5.

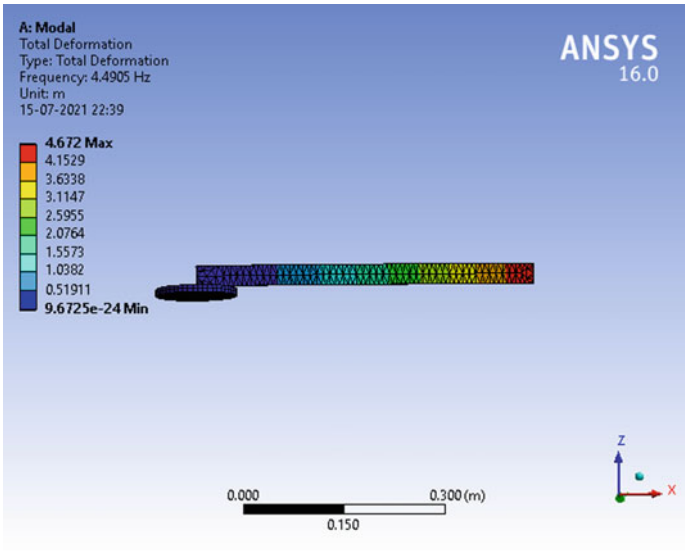

Fig. 10 First mode of the flexible-link and flexible-joint manipulator

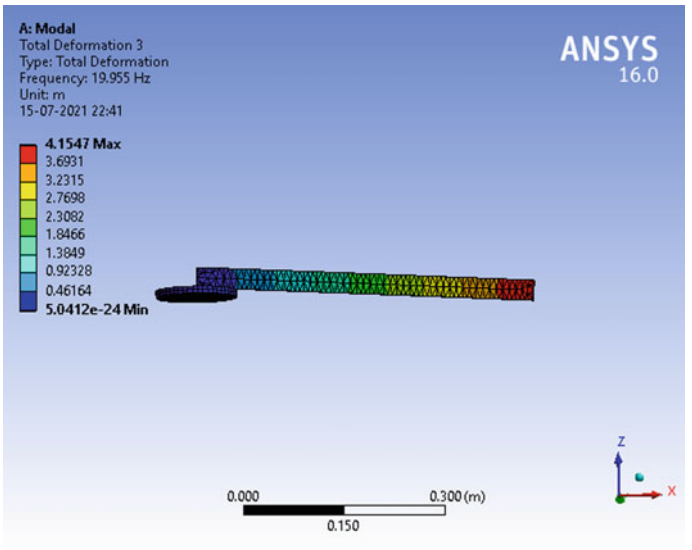

Fig. 11 Second mode of the flexible-link and flexible-joint manipulator

Table 5 Modal frequencies of vibrations of a single flexible-link flexible-joint manipulator

Mode of vibration	Frequency (Hz)
First mode	4.4905
Second mode	19.955
Third mode	28.484

3.3 *Dynamic Analysis of Curved Flexible-Link and Rigid-Joint Manipulator with Circular Holes*

Simulation has been carried out using curved flexible links and rigid joints with circular holes. Different mode shapes are shown in the figures below. In each of these cases, the natural frequencies of the flexible link tip are calculated from its equilibrium position. Figures 12 and 13 are mode shapes of curved flexible links and rigid joints with circular holes of steel material and aluminum alloy.

The first three modal frequencies with a variety of materials are given in Table 6. It is observed that aluminum alloy material gives higher natural frequencies than steel material.

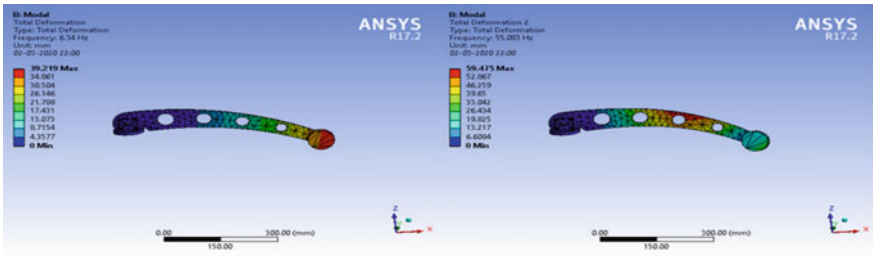

Fig. 12 First and second modes of curved flexible-link and rigid-joint manipulator with circular holes

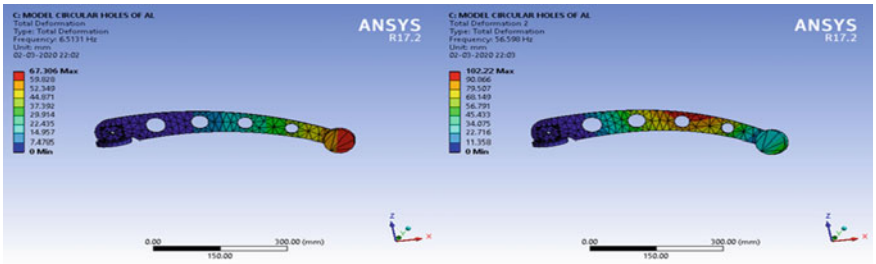

Fig. 13 First and second modes of curved flexible-link and flexible-joint manipulator with circular holes

Table 6 Mode frequencies of curved flexible link and rigid joint with circular holes

Mode shape no.	Mode frequencies (Hz)		
	Experimental [11]	Present work	Simulation of AL Alloy
1	6.251	6.34	6.5131
2	54.590	55.083	56.598
3	87.390	89.155	91.185

3.4 *Dynamic Analysis of Curved Flexible-Link and Rigid-Joint Manipulator with Different Types of Holes*

In this subsection, the curved manipulator shown in Fig. 4 is analyzed using ANSYS. Four different types of holes, viz., circular (Fig. 13), hexagonal (Fig. 14), pentagonal (Fig. 15), and rectangular (Fig. 16) have been considered, and the first two modes have been shown in the figures. Table 7 gives the modal frequencies of the first 4 modes. The results of the circular holes have been compared with those available in the literature [11] and are found to be in good agreement.

Simulation of dynamic analysis of flexible-link manipulator has been carried out using curved flexible-link and rigid-joint manipulator with hexagonal holes. Different mode shapes are shown in the figures below. In each of these cases, the natural frequencies of the flexible link are calculated from its equilibrium position. Figure 14 shows the mode shapes of a curved flexible-link and rigid-joints manipulator with hexagonal holes of steel material. Figure 15 shows the mode shapes of a curved flexible-link and rigid-joints manipulator with pentagonal holes of steel material.

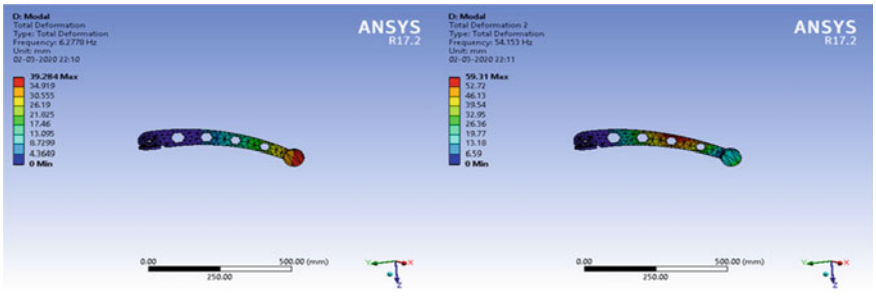

Fig. 14 First and second modes of curved flexible-link and rigid-joint manipulator with hexagonal holes

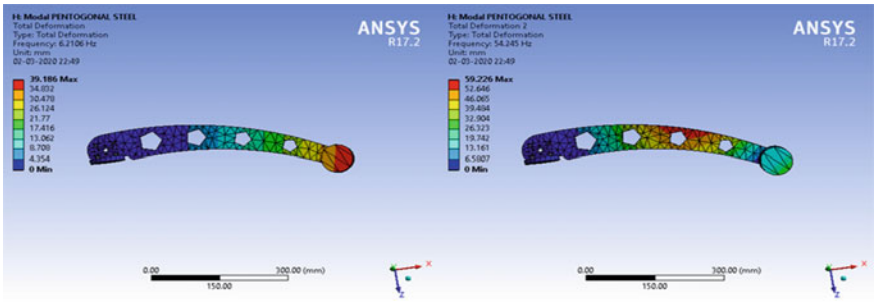

Fig. 15 First and second modes of curved flexible-link and rigid-joint manipulator with pentagonal holes

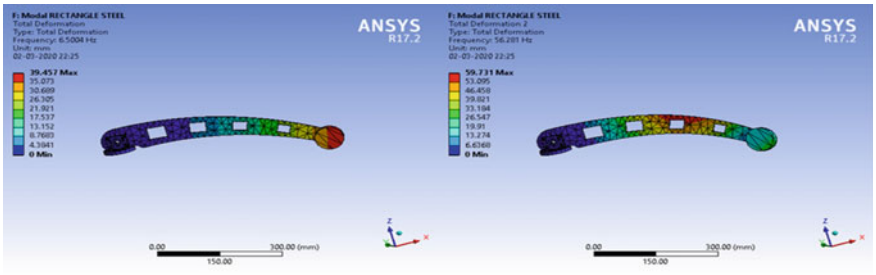

Fig. 16 First and second modes of curved flexible-link and rigid-joint manipulator with rectangular holes

Table 7 Comparison of modal natural frequencies of steel manipulator with different types of holes

Mode shape no.	Mode frequencies (Hz)			
	Circular holes [11]	Hexagonal holes	Pentagonal holes	Rectangular holes
1	6.34	6.2778	6.2106	6.5004
2	55.083	54.153	54.245	56.281
3	89.155	87.719	87.128	90.744
4	142.9	141.68	140.7	146.06

Figure 16 shows the mode shapes of a curved flexible-link and rigid-joint manipulator with rectangular holes of steel material.

The first four modal frequencies with the variation of a type of holes are given in Table 7 of steel material and aluminum alloy. It has been observed that rectangular holes give higher natural frequencies than other types of holes.

4 Conclusion

In the present paper, the modal analysis of different types of flexible-link manipulators mentioned in Sect. 3 with or without joint flexibilities has been performed in the commercial finite element software package ANSYS. The following conclusions can be drawn from the above analyses:

- The natural frequencies of the first three modes are greater in tapered flexible-link manipulators with rigid joints than in rectangular flexible-link manipulators with holes and rigid joints.
- It is noticed that the manipulator of aluminum alloy material gives greater natural frequencies than that of steel material in the first three modal frequencies of curved flexible-link and rigid-joint manipulators with circular holes.

- In the first four modal frequencies of the curved flexible-link manipulators with a variety of types of holes, the one with rectangular holes has been found to have higher natural frequencies than with other types of holes.

References

1. Dwivedy SK, Eberhard P. Dynamic analysis of flexible manipulators, a literature review. Mech Mach Theory. 2006;41(7):749–77.
2. Kiang CT, Spowage A, Yoong CK. Review of control and sensor system of flexible manipulator. J Intell Rob Syst. 2015;77(1):187–213.
3. Ankarali A, Diken H. Vibration control of an elastic manipulator link. J Sound Vib. 1997;204(1):162–70.
4. Wang FY, Guan G. Influences of rotatory inertia, shear and loading on vibrations of flexible manipulators. J Sound Vib. 1994;171(4):433–52.
5. Wang FY, Russell JL. Optimum shape construction of flexible manipulators with total weight constraint. IEEE Trans Syst Man Cybern. 1995;25(4):605–14.
6. Wang FY, Russell JL. A new approach to optimum flexible link design. In: Proceedings of 1995 IEEE international conference on robotics and automation, vol 1. IEEE, p. 931–6
7. KhalilIbrahim AAAB, Ismail AA. Mode shape analysis of a flexible robot arm. Int J Control Autom Syst 1(2)
8. Shin K, Brennan MJ. Two simple methods to suppress the residual vibrations of a translating or rotating flexible cantilever beam. J Sound Vib. 2008;312(1–2):140–50.
9. Korayem MH, Nikoobin A. Maximum payload for flexible joint manipulator in point-to-point task using optimal control approach. Int J Adv Manuf Technol. 2008;38(9–10):1045–60.
10. Malgaca L, Karagülle H. Numerical and experimental study on integration of control actions into the finite element solutions in smart structures. Shock Vib. 2009;16(4):401–15.
11. Malgaca L, Yavuz Ş, Akdağ M, Karagülle H. Residual vibration control of a single-link flexible curved manipulator. Simul Model Pract Theory. 2016;67:155–70.
12. De Luca A, Siciliano B. Inversion-based nonlinear control of robot arms with flexible links. J Guid Control Dyn. 1993;16(6):1169–76.
13. Abe A. Trajectory planning for residual vibration suppression of a two-link rigid-flexible manipulator considering large deformation. Mech Mach Theory. 2009;44(9):1627–39.
14. Spong MW. Modeling and control of elastic joint robots. J Dyn Syst Meas Contr. 1987;109:310–8. https://doi.org/10.1115/1.3143860.
15. Wei J, Cao D, Liu L, Huang W. Global mode method for dynamic modeling of a flexible-link flexible-joint manipulator with tip mass. Appl Math Model. 2017;48:787–805.